JOURNAL OF VIROLOGY, June 2006, p. 5571–5576 Vol. 80, No. 11
0022-538X/06/$08.00+0 doi:10.1128/JVI.02589-05

Influence of Pseudorabies Virus Proteins on Neuroinvasion and Neurovirulence in Mice

Robert Klopfleisch,[1,2] Barbara G. Klupp,[1] Walter Fuchs,[1] Martina Kopp,[1] Jens P. Teifke,[2] and Thomas C. Mettenleiter[1]*

Institutes of Molecular Biology[1] and Infectology,[2] Friedrich-Loeffler-Institut, 17493 Greifswald-Insel Riems, Germany

Received 13 December 2005/Accepted 15 March 2006

Neurotropism is a distinctive feature of members of the *Alphaherpesvirinae*. However, its molecular basis remains enigmatic. In the past, research has been focused mainly on the role of viral envelope proteins in modulating herpesvirus neuroinvasion and neurovirulence (T. C. Mettenleiter, Virus Res. 92:192–206, 2003). To further analyze the molecular requirements for neuroinvasion of the alphaherpesvirus pseudorabies virus (PrV), adult mice were infected intranasally with a set of single- or multiple-deletion mutants lacking the UL3, UL4, UL7, UL11, UL13, UL16, UL17, UL21, UL31, UL34, UL37, UL41, UL43, UL46, UL47, UL48, UL51, US3, US9, glycoprotein E (gE), gM, UL11/US9, UL11/UL16, UL16/UL21, UL11/UL16/UL21, UL11/gE, UL11/gM, UL43/gK, UL43/gM, or UL43/gK/gM genes. Neurovirulence was evaluated by measuring mean survival times compared to that after wild-type virus infection. Furthermore, by immunohistochemical detection of infected neurons, the kinetics of viral spread in the murine central nervous system was investigated.

In their hosts, alphaherpesviruses infect a wide range of cells. However, they also exhibit a marked neurotropism by invasion of the peripheral and central nervous systems (CNS), resulting in acute neurologic diseases and/or the establishment of latency in neurons (46a, 47, 48). Pseudorabies virus (PrV), a member of the genus *Varicellovirus*, is the causative agent of Aujeszky's disease. Pigs are considered the natural host since they are the only animal species able to survive a productive PrV infection (reviewed in reference 42). In mice, PrV shows almost exclusively neurogenic infections of the CNS with fulminant central nervous symptoms and high mortalities (27). After oronasal inoculation, which represents the natural route of infection, PrV first replicates in the nasal epithelium. It then enters free nerve endings of trigeminal as well as other sympathetic, parasympathetic, and facial nerve neurons that innervate the nasal mucosa (3). Replication in the cell bodies of first-order neurons in the trigeminal ganglion (TG) is followed by axonal transport to transsynaptically connected second-order neurons in the afferent trigeminal nuclei of the brain stem, which are the spinal trigeminal nucleus (Sp5), the mesencephalic trigeminal nucleus (Me5), and the principal sensory trigeminal nucleus (Pr5) (49). If the mice survive beyond that point, the virus is carried on to synaptically connected neuronal centers like the cerebral cortex.

Herpesvirus particles consist of four separate morphological components, the inner nucleoprotein core, the icosahedral capsid, the tegument, and the envelope (43). In the past, the influence of PrV envelope proteins on viral neuroinvasion and neurovirulence has been analyzed thoroughly (1–3, 6, 7, 17, 44). However, knowledge about the role of other structural and nonstructural viral proteins in neuroinvasion is sketchy (18, 20, 21, 27, 31, 32, 44). In the present work, we describe and summarize the influence of the deletion of several tegument, membrane-associated, and nonstructural proteins on neuroinvasion and neurovirulence of PrV in mice.

* Corresponding author. Mailing address: Institute of Molecular Biology, Friedrich-Loeffler-Institut, Boddenblick 5A, D-17493 Greifswald-Insel Riems, Germany. Phone: 49-38351-7250. Fax: 49-38351-7151. E-mail: thomas.mettenleiter@fli.bund.de.

MATERIALS AND METHODS

Viruses and cells. The virus mutants used in this study were derived from PrV strain Kaplan (PrV-Ka) (26). PrV-Ka was used as the wild-type control, and the live attenuated vaccine strain Bartha (PrV-Ba) was included as a virus with a specific defect in anterograde spread (4, 9). The construction of deletion mutants PrV-ΔUL3 (31), PrV-ΔUL4 (W. Fuchs et al., submitted for publication), PrV-ΔUL7 (18), PrV-ΔUL11 (39), PrV-ΔUL16 (29), PrV-ΔUL17 (32), PrV-ΔUL21 (29), PrV-ΔUL31 (22), PrV-ΔUL34 (30), PrV-ΔUL37 (35), PrV-ΔUL43 (28), PrV-ΔUL46 (40), PrV-ΔUL47 (40), PrV-ΔUL48 (19), PrV-ΔUL51 (33), PrV-ΔUS3 (34), PrV-ΔgE (38), PrV-ΔgM (38), PrV-ΔUL11/UL16 (29), PrV-ΔUL16/UL21 (29), PrV-ΔUL11/UL16/UL21 (29), PrV-ΔUL11/gE (38), PrV-ΔUL11/gM (38), PrV-ΔUL43/gK (28), PrV-ΔUL43/gM (28), respective rescuants, and complementing cell lines have been described elsewhere. Viruses were grown and titrated in permanent porcine kidney cells or complementing rabbit kidney (RK13) cells (for mutants lacking UL17, UL11/gM, UL31, UL34, UL37, or UL43/gK/gM).

Generation of US9 deletion mutants and rescuants. For the creation of mutant PrV-ΔUS9F, a 285-bp AflIII fragment containing codons 4 to 97 of the US9 gene was removed by Red recombinase-mediated mutagenesis of the genome of PrV-Ka cloned as a bacterial artificial chromosome in *Escherichia coli* as described previously (10, 12, 39), followed by flp-recombinase-mediated excision of the inserted selection marker, the kanamycin resistance gene (KanR), retaining one copy, i.e., 36 bp, of the flp-recombinase recognition target (FRT) sequence. A US9 and UL11 double-negative mutant was derived from pPrV-ΔUL11F, which already contained an FRT site at the UL11 locus (39). In this case, a KanR gene without additional FRT sites was permanently inserted at the US9 locus to avoid undesired recombination events. Since US9 forms a 3′ coterminal transcription unit with the upstream US8 gene encoding glycoprotein (gE) (36), an artificial polyadenylation signal was introduced downstream of US8 to avoid the impairment of gE expression by the US9 mutation. Finally, the bacterial vector sequences at the gB loci of pPrV-ΔUS9F and pPrV-ΔUL11F/ΔUS9K were replaced by the authentic PrV gB gene after calcium-phosphate-mediated cotransfection of RK13 cells with bacterial artificial chromosome and plasmid DNA as described previously (23, 24, 39). US9 rescue mutants were isolated after cotransfection with a cloned 4,623-bp BamHI/SalI subfragment of BamHI fragment 7, which contains the US9 gene, and dot blot hybridization. Immunofluorescence and immunoblotting using a rabbit anti-US9 antiserum (kindly provided by L.W. Enquist, Princeton, N.J.) and an anti-UL11 antiserum (39) were used to verify the absence of the US9 and/or UL11 proteins (data not shown).

Construction of PrV-ΔUL13β. For the construction of a mutant lacking codons 17 to 352 of the UL13 gene, regions up- and downstream of the open reading frame were amplified by PCR from BamHI fragment 3 using *pfx* DNA polymerase (Invitrogen) and primers UL14for (5′-CACAAAGCTTCGGTGGC GCGCTCGGCG-3′; nucleotides [nt] 76336 to 76352; accession no. BK001744 [36]) and UL14rev (5′-CACAGTCGACGCGCCAGCGCGGCCCG-3′; nt 77561 to 77546; accession no. BK001744) as well as UL12for (5′-CACAGGATCCCTGGC CGCCGGCTTCCGC-3′; nt 78569 to 78586; accession no. BK001744) and UL12rev (5′-CACAGAATTCGGGGCCGGGCTCGCCGAC-3′; nt 80209 to 80192; accession no. BK001744) (underlined are HindIII/SalI sites for the UL14 region and BamHI/EcoRI sites for the UL12 region). The PCR products were cleaved with the corresponding restriction enzymes for which recognition sites were introduced with the primers and subsequently cloned into the appropriately cleaved vector pUC19 (New England Biolabs). The SalI and BamHI sites were then used for the introduction of a BamHI/SalI β-galactosidase expression cassette (45). The resulting plasmid pUC-ΔUL13β was cotransfected with PrV-Ka DNA into RK13 cells by calcium phosphate coprecipitation (24). Plaques which were stained blue under a BluoGal overlay were picked by aspiration and further purified to homogeneity. One plaque isolate, named PrV-ΔUL13β, was randomly selected for further analysis. The UL13 rescue mutant PrV-ΔUL13R was isolated after the cotransfection of RK13 cells with DNA of PrV-ΔUL13β and a plasmid containing a genomic 5.1-kb SalI/KpnI fragment of PrV-Ka DNA (nt 75781 to 80874; accession no. BK001744) comprising the UL14 to UL11 gene region (36).

Generation of PrV-ΔUL41 and PrV-ΔUL41R. For the generation of a mutant lacking codons 21 to 349 of the UL41 gene, a 3.9-kb BstXI subfragment of BamHI fragment 2 containing the complete UL41 open reading frame and flanking regions was cloned after blunt-end treatment with T4 DNA polymerase into SmaI-cleaved vector pUC19 (NEB). UL41 flanking regions were PCR amplified by *pfx* polymerase using primers UL41d1 (5′-CACAAAGCTTCTCCGC CGCGGACGACCTC-3′; nt 49154 to 49172; accession no. BK001744) and UL41d2 (5′-CACAGGATCCACCAGGCCGTCCTCATGGCG-3′; nt 50456 to 50437; accession no. BK001744) as well as UL41d3 (5′-CACAGGTACCGCCT CCGAGCGCCCAGACG-3′; nt 51440 to 51459; accession no. BK001744) and UL41d4 (5′-CACAGAATTCGACCCCCGGCGCTGGAGGAG-3′; nt 52320 to 52304; accession no. BK001744). The resulting PCR fragments were cleaved with restriction enzymes for which recognition sites were provided by the respective primers (underlined), i.e., HindIII and BamHI for fragment ΔUL41 1-2 and KpnI and EcoRI for ΔUL41 3-4. Both PCR fragments were subsequently cloned into appropriately cleaved vector pUC19, resulting in plasmid pUC-ΔUL41 d1-4. Between both PCR fragments a BamHI/KpnI green fluorescent protein expression cassette was inserted. Sequencing of the cloned PCR products revealed that the product of UL41 d1/2 was shorter than expected and ended at nucleotide position 50369 instead of 50456. However, for the generation of the UL41 deletion mutant, this was of no relevance and ignored. Subsequently, pUC-ΔUL41GFP was cotransfected with genomic DNA of PrV-Ka into RK13 cells. Green fluorescent plaques were picked and purified to homogeneity, and one plaque isolate, PrV-ΔUL41G, was further studied. A UL41 rescuant, PrV-ΔUL41R, was generated by cotransfection of RK13 cells with PrV-ΔUL41G viral DNA and plasmid pUC-BstXI3.9 followed by the isolation of nonfluorescent plaques.

Generation of PrV-ΔgK/43G/Mβ. For the generation of a mutant simultaneously lacking UL43, gK and gM DNA of PrV-ΔgK/UL43G (28) was cotransfected with plasmid pΔUL10β (15) into RK13-gK cells (13) and transfection progeny was screened for blue plaque phenotypes. One isolate, designated PrV-ΔgK/43G/Mβ, was further characterized.

Determination of plaque size and one-step growth analysis. For the determination of plaque sizes, RK13 cells were infected with the different viruses and incubated for 2 days in semisolid medium. Subsequently, cells were fixed with 5% formalin and stained with crystal violet. For each virus strain, 30 to 50 plaques were measured microscopically in three independent experiments and the plaque diameter was determined relative to the plaque size of PrV-Ka, which was set at 100%. To monitor kinetics of viral replication, RK13 cells were infected with a multiplicity of infection of 5 for 1 h at 4°C. By replacing the inoculum with prewarmed medium, the virus was allowed to penetrate for 1 h at 37°C. Nonpenetrated virus was inactivated by a low-pH treatment (41). After incubation for 0, 4, 8, 12, 24, and 36 h at 37°C, infected cells and supernatant were removed and plated in serial dilutions onto RK13 cells. Final titers were recorded at 36 h postinfection (p.i.).

Animal experiments. The influence of the deletions on viral neuroinvasion was investigated in a mouse model as described previously (27). For all experiments, 6- to 8-week-old CD1 mice were used. To analyze mean survival times, 10 animals were inoculated with each of the various deletion mutants or PrV-Ka and 3 animals were inoculated with each of the rescue mutants. Five microliters of the respective virus suspension containing 10^6 PFU was intranasally instilled bilaterally into anesthetized mice as described previously (27). Animals were observed twice a day for a period of 14 days or euthanized for animal welfare reasons when severe clinical symptoms were observed (27). The kinetics of viral spread were investigated by the euthanasia of an additional three mice every 24 h after inoculation. After necropsy, the head, including brain and trigeminal ganglia, and the spinal cord were fixed in neutral buffered 4% paraformaldehyde. Fixed tissues were embedded in Histosec (Merck) and cut in transversal serial paraffin sections. Immunohistochemistry was performed to detect the PrV antigen in paraffin sections. To this end, a rabbit antiserum specific for the PrV major capsid protein, the UL19 gene product, was used (27). For the visualization of antibody binding, the avidin-biotin complex method was performed (25). Parallel sections of healthy mice were used as antigen-negative tissue controls to monitor the specificity of the rabbit anti-UL19 serum. The location of the infected nuclei in the brain stem and pons was determined according to the method of Paxinos and Franklin (46).

RESULTS

Neurovirulence and kinetics of viral spread of PrV-Ka. The inoculation with PrV-Ka led to a mean time to death of 49 h p.i. (Table 1), which was highly reproducible (27). PrV UL19 antigen was detectable in respiratory epithelial cells of the nasal mucosa and in first-order trigeminal neurons (trigeminal ganglia) at 24 h p.i. (see Fig. 2). The infection of second-order trigeminal neurons of the brain stem and the pons was detectable at 49 h p.i. PrV antigen was found mainly in the caudal part of the trigeminal nucleus (Sp5C; bregma −5.68 to −8.24) and in the mesencephalic (Me5; bregma −4.16 to −5.20) and pontine (Pr5; bregma −4.84 to −5.68) trigeminal nuclei. Besides the infection of neurons of the trigeminal circuit, an infection of sympathetic neurons in the cervical cranial ganglion (GCC) and of parasympathetic neurons in the pterygopalatinum ganglion (GPP) was observed in all mice at 49 h p.i. Furthermore, neurons of the facial nucleus (NF; bregma −5.68 to −6.48) and the solitary tract nucleus (bregma −6.24 to −8.24) were infected constantly at 49 h p.i. No antigen was detectable in neurons of the ventral posteriomedial thalamic nucleus (VPM; bregma −1.06 to −2.54) or neurons of the ectorhinal (ECT, bregma 0.98 to −1.82) and lateral entorhinal (LENT, bregma −2.90 to −3.80) cortex. In sections of the lung, liver, spleen, kidney, and heart no viral antigen was detectable.

Analysis of PrV mutants deleted in UL3, UL4, gM, UL11, UL13, UL21, UL41, UL43, UL43/gM, UL46, UL47, UL51, and US3. Deletion of these genes resulted in increased mean times to death ranging between 51 and 71 h p.i. (Fig. 1 and Table 1), which correlates with a slower neuroinvasion. Trigeminal first-order neurons were found infected between 1 and 2 days p.i, and second-order neurons were found infected between 2 and 3 days p.i. Additionally, the infection of NF, GCC, and GPP was found from 2 days p.i. onwards. However, neurons of the cerebral cortex and the VPM remained uninfected. Thus, the deletion of these genes had a slight to moderate influence on neuroinvasion and neurovirulence.

Analysis of PrV mutants deleted in UL7, UL16, UL48, US9, gE, UL11/UL16, UL16/UL21, UL11/UL16/UL21, UL11/US9, UL11/gE, and UL43/gK. In mutant viruses lacking UL7, US9, or gE, the mean time to death ranged between 70 and 72 h (Fig. 1 and Table 1). However, in mice infected with these mutants, in addition to cells in the nasal respiratory epithelium, the TG (2 days p.i.), and the Sp5C (3 days p.i.), PrV antigen was also detectable in single neurons of the VPM and the

TABLE 1. Mean time to death and time points of appearance of PrV UL19 antigen in mice infected experimentally with PrV-Ka, PrV-Ba, and PrV deletion mutants[a]

PrV	Titer reduction[b]	Plaque size[c] (%)	Mean time to death, hours p.i.[d]	IHC positive at indicated day p.i.[e]			
				Nasal cavity	First-order neurons	Second-order neurons	ECT/ LENT
Ka		100	49 (1.6)	1	1	2	—
Ba	5	50	100 (2.3)	1	2	3	5
ΔUL3	0	100	51 (1.6)	1	1	2	—
ΔUL4	5	100	54 (3.3)	1	1	2	—
ΔUL7	10	40	70 (3.2)	1	2	3	3
ΔUL11	10	40	67 (1.7)	1	2	3	—
ΔUL13	10	80	57 (1.5)	1	2	2	—
ΔUL16	10	35	81 (2.6)	1	2	3	4
ΔUL17	10^4	10	>336	1	—	—	—
ΔUL21	10	50	71 (1.6)	1	2	3	—
ΔUL31	10^2	20	>336	1	—	—	—
ΔUL34	5×10^2	20	>336	1	—	—	—
ΔUL37	10^2	50	>336	1	—	—	—
ΔUL41	10	80	68 (2.1)	1	2	3	—
ΔUL43	5	90	52 (1.8)	1	1	2	—
ΔUL46	0	70	51 (2.0)	1	1	2	—
ΔUL47	10	70	57 (1.8)	1	2	2	—
ΔUL48	10^3	40	126 (3.8)	1	3	4	5
ΔUL51	10	30	64 (1.4)	1	2	3	—
ΔUS3	10	90	56 (1.6)	1	2	2	—
ΔUS9	10	100	72 (3.0)	1	2	3	3
ΔgE	0	70	72 (2.3)	1	2	3	3
ΔgM	50	80	62 (1.8)	1	2	3	—
ΔUL11/US9	10	40	122 (3.3)	1	3	4	5
ΔUL11/UL16	50	40	83 (1.8)	1	2	3	4
ΔUL16/UL21	10^2	40	131 (5.6)	1	3	4	5
ΔUL11/UL16/UL21	10^2	40	137 (5.29)	1	3	4	5
ΔUL11/gE	10	90	122 (3.2)	1	3	4	5
ΔUL11/gM	10^3	5	>336	1	—	—	—
ΔUL43/gK	10^2	10	140 (5.5)	1	3	4	5
ΔUL43/gM	50	80	63 (1.9)	1	2	2	—
ΔUL43/gK/gM	5×10^2	10	>336	1	—	—	—

[a] Nasal cavity: respiratory mucosal epithelium; first-order neurons: trigeminal ganglion; second-order neurons: spinal trigeminal nucleus (Sp5), mesencephalic trigeminal nucleus (Me5), and principal sensory trigeminal nucleus (Pr5); ECT/LENT, ectorhinal/lateral entorhinal cortex.
[b] The reduction in titer (*n*-fold) on RK13 cells compared to titers of wild-type PrV-Ka is indicated.
[c] Plaque sizes on RK13 cells are indicated compared to those of wild-type PrV-Ka, which had been set as 100%.
[d] Mean time to death is given. Numbers in brackets indicate standard deviations.
[e] Kinetics of infection as analyzed by immunohistochemistry (IHC). Given are the numbers of days p.i. when PrV antigen-positive cells were first observed. —, virus infection did not reach this neuronal level.

LENT and ECT cortex after 3 days. Apparently, around 70 h p.i. is a critical time point since in animals that survived for this period of time, infection was able to reach the cerebral cortex (Table 1). This extent of neuroinvasion had not been observed with either the wild-type PrV-Ka or the mutant viruses described above.

Animals infected with mutants lacking UL16 or UL11/16 exhibited a mean time to death of 81 or 83 h, respectively (Fig. 1 and Table 1). Thus, the additional deletion of UL11 did not significantly increase the mean time to death and did not change the anatomical pattern of neuroinvasion beyond that of the UL16 single deletion. Apparently, the effects of single deletions of UL11 and UL16 do not cumulate in the double deletion, indicating that both may be involved in a similar function in PrV neuroinvasion. The same is true for plaque sizes in vitro (Table 1), whereas titers in cell culture decreased a further fivefold in the absence of both proteins over the single-deletion mutants (Table 1). CNS infection also reached the cerebral cortex after 4 days p.i. This demonstrates that these mutants possess neuroinvasive potential which allows them to travel to higher areas of the brain. In contrast, PrV-Ka is not able to reach these higher neuronal centers due to early death of the animals. Strictly speaking, the less neurovirulent the viruses are, the higher their neuroinvasiveness. Mice infected with PrV-Ba survived on average to 100 h p.i. The kinetics of viral invasion of the CNS and distribution of viral antigen were similar to those observed with the PrV mutants described above.

The increase in neuroinvasion was even more pronounced in the mutants PrV-ΔUL48, PrV-ΔUL11/US9, PrV-ΔUL16/UL21, PrV-ΔUL11/UL16/UL21, PrV-ΔUL11/gE, and PrV-ΔUL43/gK. Mean survival times ranged from 122 to 140 h p.i., which was even higher than that observed after infection with the live attenuated vaccine strain PrV-Ba (Fig. 1). In mice infected with these mutants, the entry into neuronal circuits and establishment of an infection of first-order neurons was significantly delayed. Infection of the TG, GCC, GPP, or NF was observed only after 3 days p.i. and, thus, 48 h later than after infection with wild-type PrV-Ka. Again, thalamic neurons were infected slightly later at 4 days p.i. Cerebral neurons of

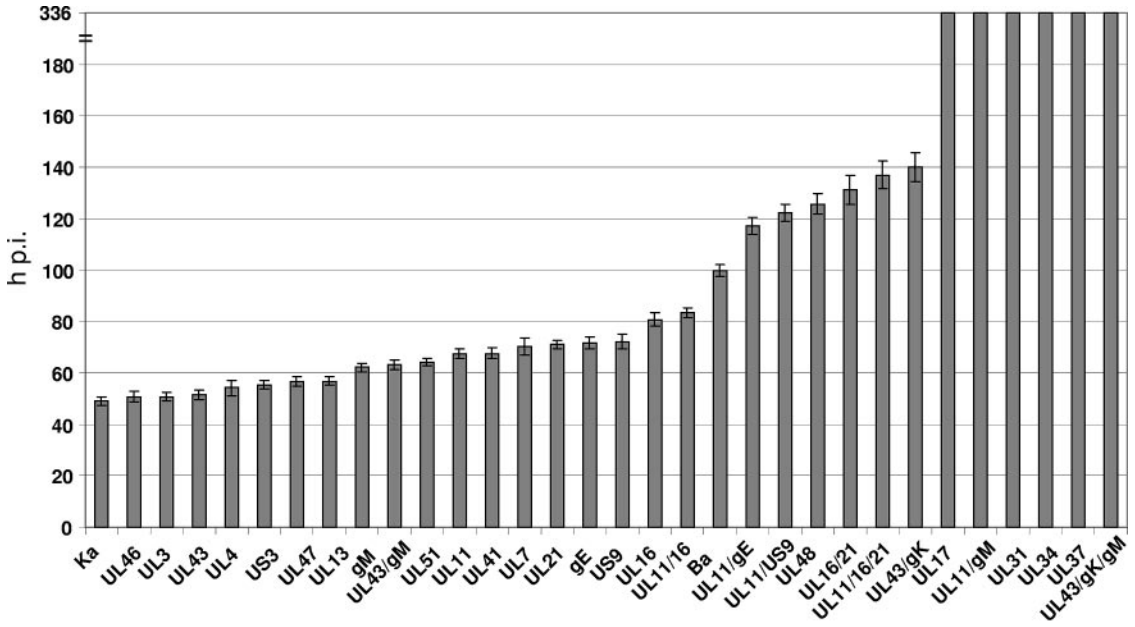

FIG. 1. Mean survival times of mice ($n = 10$) that were inoculated intranasally with 10^6 PFU of the respective virus strain. Mice were observed for a maximum of 336 h p.i. Standard deviations are indicated by error bars.

the ECT and LENT were invariably found infected at 5 days p.i. (Fig. 2), which supports the previous finding of an inverse correlation between neurovirulence and neuroinvasiveness.

Analysis of mutants devoid of UL17, UL31, UL34, UL37, UL11/gM and UL43/gK/gM. Mutant viruses lacking UL17, UL31, UL34, UL37, UL11/gM, or UL43/gK/gM genes exhibited titer reductions in cell culture of between 100- and 10,000-fold, necessitating the use of complementing cells for productive replication in vitro. This already indicated that the missing gene products are very important for viral replication. The

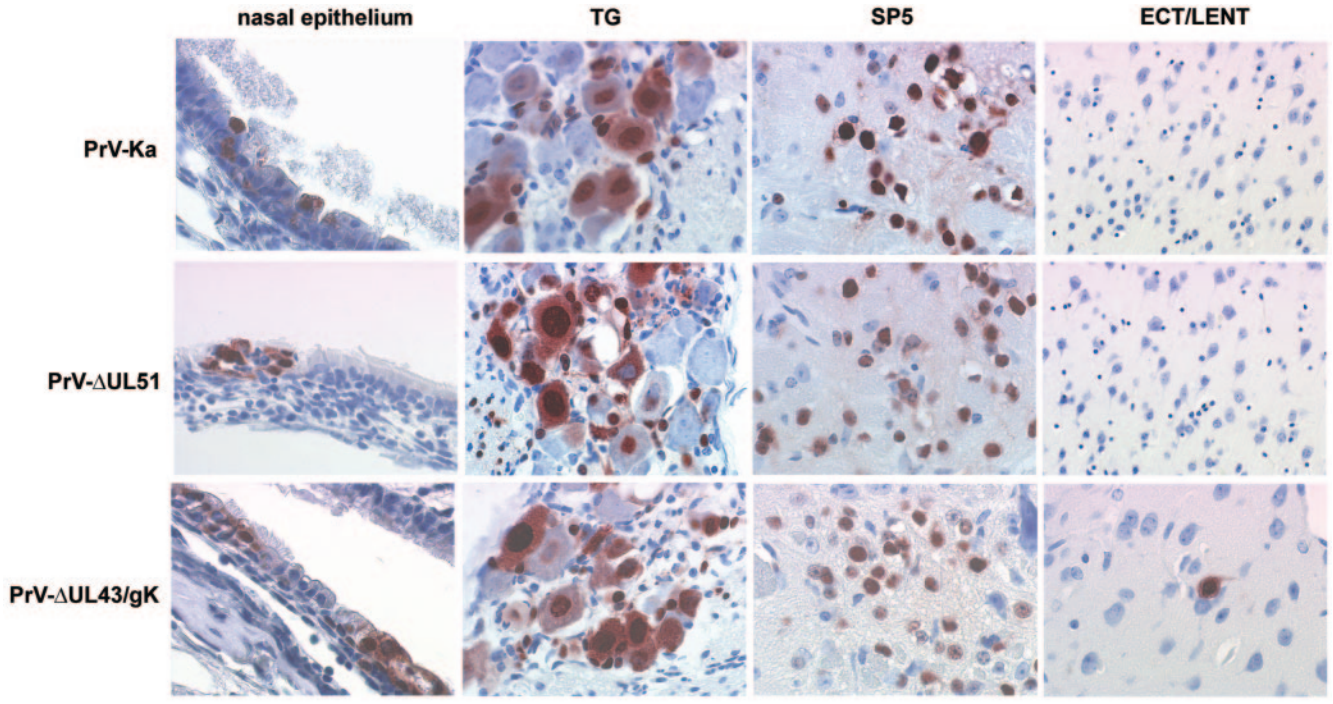

FIG. 2. Immunohistochemistry for the detection of PrV UL19 antigen in mice after intranasal inoculation with PrV-Ka, PrV-ΔUL51, and PrV-ΔUL43/gK in the nasal epithelium, trigeminal ganglion, spinal trigeminal nucleus, and the ectorhinal and lateral entorhinal cortex at mean time to death. No differences in the extent of neuronal infection in the TG or Sp5 were observed. Magnification, ×150.

observed in vitro replication defects of these mutants parallel their inability to produce clinical symptoms within the observed time period of 14 days p.i. after intransal infection of the mice. By histological examination, single infected nasal epithelial cells were observed, but no antigen was detectable in neurons (data not shown). Thus, the lack of neuroinvasion and neurovirulence correlated with the defects of these mutants during replication in cell culture. Obviously, the requirement for these gene products is similar in vitro and in vivo. However, it is interesting to note that several mutant viruses with similar reductions in titers in vitro, such as PrV-ΔUL16/UL21, PrV-ΔUL11/UL16/UL21, PrV-ΔUL43/gK, or PrV-ΔUL48, were still able to invade the CNS and the infected mice succumbed to the infection. Thus, it will be interesting in future experiments to directly compare mutant virus pairs with similar in vitro, but different in vivo, phenotypes.

Rescue mutants. Inoculation of the mice with rescuants of all single-deletion mutants led to mean times to death of between 49 to 52 h p.i. The kinetics of viral invasion of the CNS as well as the infected neuronal centers were identical to those observed with PrV-Ka (see above).

DISCUSSION

In this work, we provide a comprehensive evaluation of the neuroinvasive properties and the kinetics of transsynaptic propagation of a wide range of PrV deletion mutants in structural and nonstructural proteins in the mouse by analysis of mean survival times and immunohistochemistry studies. For most of the mutants, a more or less striking defect in viral replication in nonneuronal cells in culture was found to correlate with a proportional increase in survival times (5, 14, 18, 22, 28, 30, 33–35, 37–40) (Table 1). We demonstrate that most of the analyzed deletions only slightly hampered neuroinvasion and neurovirulence. Nevertheless, several deletion mutants displayed a marked attenuation or a total block of neurovirulence. As reported earlier, the decrease in neurovirulence in most cases was inversely proportional to the capacity for neuroinvasion (16).

Intranasal inoculation of the mice resulted in exclusive infection of nasal and pharyngeal epithelial cells but not of cells in the tracheal or pulmonary mucosa (data not shown). This led to an infection of neurons of the sympathetic, parasympathetic, facial and trigeminal circuits. Therefore, our infection model does not allow differentiation between anterograde and retrograde spread. PrV-Ba as well as PrV mutants lacking gE or US9 are known to be deficient specifically in anterograde spread (1, 6, 9, 16) but exhibited no differences in the distribution and kinetics of viral spread compared to those of several other mutant viruses after intranasal inoculation. Other in vitro and animal models like the trichamber tissue culture system or intraocular or cutaneous murine flank inoculation models need to be used to investigate whether the observed defects in neuroinvasion are specific for either retrograde or anterograde movements (6, 8, 11). A loss of virus after inoculation by sneezing or swallowing was either not present or did not influence the outcome of the experiment since mean times to death were surprisingly constant, with only marginal standard deviations, and kinetics as well as pattern of neuroinvasion within the respective groups were highly reproducible.

Taken together with the in vitro data, for most of the mutants, the delay of viral spread to the different neuronal levels of the trigeminal circuit seems to be caused by a defective viral replication in neurons. Nevertheless, several mutants, especially PrV-ΔUL11/US9, PrV-ΔUL11/gE, PrV-ΔUL11/UL16/UL21, PrV-ΔUL43/gK, and PrV-ΔUL48, showed a phenotype in neuroinvasion that was not anticipated from their in vitro behavior. PrV-ΔUL11/US9 and PrV-ΔUL11/gE were only slightly impaired in vitro but exhibited a significantly increased mean time to death in vivo. Relative to PrV-ΔUL31, PrV-ΔUL34, PrV-ΔUL37, and PrV-ΔUL43/gK/gM, the deletion mutants PrV-ΔUL11/UL16/UL21, PrV-ΔUL43/gK, and PrV-ΔUL48 were comparably impaired in vitro but in contrast to the former were still able to enter and spread in the CNS. In these cases, neuron-specific effects in axonal transport, transsynaptic spread, or possibly immune response or induction of neuronal apoptosis might influence these in vivo phenotypes. So far, for only gE has a direct function in promoting clinical symptoms and death been described (50) and US9 has been shown to be involved in axonal transport of virions (51).

The neuroinvasion of deletion mutants in the UL17, UL31, UL34, UL37, UL11/gM, and UL43/gK/gM genes was blocked completely. This correlated well with the observations that these mutants showed severe defects in replication and intercellular spread in vitro. Although all of them were able to infect at least individual respiratory epithelial cells, none of them were able to overcome the epithelial barrier and establish a productive infection of neuronal tissue. Thus, the presence of these proteins is essential for neurovirulence in mice.

Further investigations are in progress to analyze in detail the molecular mechanisms of the contribution of the other proteins on neuroinvasion and neurovirulence of PrV.

ACKNOWLEDGMENT

This study was supported by a grant from the Deutsche Forschungsgemeinschaft (DFG Me 854/9-1).

REFERENCES

1. **Babic, N., B. Klupp, A. Brack, T. C. Mettenleiter, G. Ugolini, and A. Flamand.** 1996. Deletion of glycoprotein gE reduces the propagation of pseudorabies virus in the nervous system of mice after intranasal inoculation. Virology **219:**279–284.
2. **Babic, N., T. C. Mettenleiter, A. Flamand, and G. Ugolini.** 1993. Role of essential glycoproteins gII and gp50 in transneuronal transfer of pseudorabies virus from the hypoglossal nerves of mice. J. Virol. **67:**4421–4426.
3. **Babic, N., T. C. Mettenleiter, G. Ugolini, A. Flamand, and P. Coulon.** 1994. Propagation of pseudorabies virus in the nervous system of the mouse after intranasal inoculation. Virology **204:**616–625.
4. **Bartha, A.** 1961. Experimental reduction of virulence of Aujeszky's disease virus. Magy. Allatorv. Lapja **16:**42–45.
5. **Brack, A. R., B. G. Klupp, H. Granzow, R. Tirabassi, L. W. Enquist, and T. C. Mettenleiter.** 2000. Role of the cytoplasmic tail of pseudorabies virus glycoprotein E in virion formation. J. Virol. **74:**4004–4016.
6. **Brideau, A. D., J. P. Card, and L. W. Enquist.** 2000. Role of pseudorabies virus Us9, a type II membrane protein, in infection of tissue culture cells and the rat nervous system. J. Virol. **74:**834–845.
7. **Brideau, A. D., M. G. Eldridge, and L. W. Enquist.** 2000. Directional transneuronal infection by pseudorabies virus is dependent on an acidic internalization motif in the Us9 cytoplasmic tail. J. Virol. **74:**4549–4561.
8. **Brittle, E. E., A. E. Reynolds, and L. W. Enquist.** 2004. Two modes of pseudorabies virus neuroinvasion and lethality in mice. J. Virol. **78:**12951–12963.
9. **Card, J. P., M. E. Whealy, A. K. Robins, R. Y. Moore, and L. W. Enquist.** 1991. Two alpha-herpesvirus strains transported differentially in the rodent visual system. Neuron **6:**957–969.
10. **Cherepanov, P. P., and W. Wackernagel.** 1995. Gene disruption in Escherichia coli: TcR and KmR cassettes with the option of Flp-catalyzed excision of the antibiotic-resistance determinant. Gene **158:**9–14.

11. **Ch'ng, T. H., and L. W. Enquist.** 2005. An in vitro system to study transneuronal spread of pseudorabies virus infection. Vet. Microbiol. **113:**193–197.
12. **Datsenko, K. A., and B. L. Wanner.** 2000. One-step inactivation of chromosomal genes in Escherichia coli K-12 using PCR products. Proc. Natl. Acad. Sci. USA **97:**6640–6645.
13. **Dietz, P., B. G. Klupp, W. Fuchs, B. Köllner, E. Weiland, and T. C. Mettenleiter.** 2000. Pseudorabies virus glycoprotein K requires the UL20 gene product for processing. J. Virol. **74:**5083–5090.
14. **Dijkstra, J. M., A. Brack, A. Jöns, B. G. Klupp, and T. C. Mettenleiter.** 1998. Different point mutations within the conserved N-glycosylation motif of pseudorabies virus glycoprotein M result in expression of a nonglycosylated form of the protein. J. Gen. Virol. **79:**851–854.
15. **Dijkstra, J. M., N. Visser, T. C. Mettenleiter, and B. G. Klupp.** 1996. Identification and characterization of pseudorabies virus glycoprotein gM as a nonessential virion component. J. Virol. **70:**5684–5688.
16. **Enquist, L. W.** 2002. Exploiting circuit-specific spread of pseudorabies virus in the central nervous system: insights to pathogenesis and circuit tracers. J. Infect. Dis. **186**(Suppl. 2)**:**S209–S214.
17. **Flamand, A., T. Bennardo, N. Babic, B. G. Klupp, and T. C. Mettenleiter.** 2001. The absence of glycoprotein gL, but not gC or gK, severely impairs pseudorabies virus neuroinvasiveness. J. Virol. **75:**11137–11145.
18. **Fuchs, W., H. Granzow, R. Klopfleisch, B. G. Klupp, D. Rosenkranz, and T. C. Mettenleiter.** 2005. The UL7 gene of pseudorabies virus encodes a nonessential structural protein which is involved in virion formation and egress. J. Virol. **79:**11291–11299.
19. **Fuchs, W., H. Granzow, B. G. Klupp, M. Kopp, and T. C. Mettenleiter.** 2002. The UL48 tegument protein of pseudorabies virus is critical for intracytoplasmic assembly of infectious virions. J. Virol. **76:**6729–6742.
20. **Fuchs, W., H. Granzow, and T. C. Mettenleiter.** 2003. A pseudorabies virus recombinant simultaneously lacking the major tegument proteins encoded by the UL46, UL47, UL48, and UL49 genes is viable in cultured cells. J. Virol. **77:**12891–12900.
21. **Fuchs, W., B. G. Klupp, H. Granzow, and T. C. Mettenleiter.** 2004. Essential function of the pseudorabies virus UL36 gene product is independent of its interaction with the UL37 protein. J. Virol. **78:**11879–11889.
22. **Fuchs, W., B. G. Klupp, H. Granzow, N. Osterrieder, and T. C. Mettenleiter.** 2002. The interacting UL31 and UL34 gene products of pseudorabies virus are involved in egress from the host-cell nucleus and represent components of primary enveloped but not mature virions. J. Virol. **76:**364–378.
23. **Fuchs, W., and T. C. Mettenleiter.** 1999. DNA sequence of the UL6 to UL20 genes of infectious laryngotracheitis virus and characterization of the UL10 gene product as a nonglycosylated and nonessential virion protein. J. Gen. Virol. **80:**2173–2182.
24. **Graham, F. L., and A. J. van der Eb.** 1973. A new technique for the assay of infectivity of human adenovirus 5 DNA. Virology **52:**456–467.
25. **Hsu, S. M., L. Raine, and H. Fanger.** 1981. Use of avidin-biotin-peroxidase complex (ABC) in immunoperoxidase techniques: a comparison between ABC and unlabeled antibody (PAP) procedures. J. Histochem. Cytochem. **29:**577–580.
26. **Kaplan, A. S., and A. E. Vatter.** 1959. A comparison of herpes simplex and pseudorabies viruses. Virology **7:**394–407.
27. **Klopfleisch, R., J. P. Teifke, W. Fuchs, M. Kopp, B. G. Klupp, and T. C. Mettenleiter.** 2004. Influence of tegument proteins of pseudorabies virus on neuroinvasion and transneuronal spread in the nervous system of adult mice after intranasal inoculation. J. Virol. **78:**2956–2966.
28. **Klupp, B. G., J. Altenschmidt, H. Granzow, W. Fuchs, and T. C. Mettenleiter.** 2005. Identification and characterization of the pseudorabies virus UL43 protein. Virology **334:**224–233.
29. **Klupp, B. G., S. Böttcher, H. Granzow, M. Kopp, and T. C. Mettenleiter.** 2005. Complex formation between the UL16 and UL21 tegument proteins of pseudorabies virus. J. Virol. **79:**1510–1522.
30. **Klupp, B. G., H. Granzow, and T. C. Mettenleiter.** 2000. Primary envelopment of pseudorabies virus at the nuclear membrane requires the UL34 gene product. J. Virol. **74:**10063–10073.
31. **Klupp, B. G., H. Granzow, W. Fuchs, E. Mundt, and T. C. Mettenleiter.** 2004. Pseudorabies virus UL3 gene codes for a nuclear protein which is dispensable for viral replication. J. Virol. **78:**464–472.
32. **Klupp, B. G., H. Granzow, A. Karger, and T. C. Mettenleiter.** 2005. Identification, subviral localization, and functional characterization of the pseudorabies virus UL17 protein. J. Virol. **79:**13442–13453.
33. **Klupp, B. G., H. Granzow, R. Klopfleisch, W. Fuchs, M. Kopp, M. Lenk, and T. C. Mettenleiter.** 2005. Functional analysis of the pseudorabies virus UL51 protein. J. Virol. **79:**3831–3840.
34. **Klupp, B. G., H. Granzow, and T. C. Mettenleiter.** 2001. Effect of the pseudorabies virus US3 protein on nuclear membrane localization of the UL34 protein and virus egress from the nucleus. J. Gen. Virol. **82:**2363–2371.
35. **Klupp, B. G., H. Granzow, E. Mundt, and T. C. Mettenleiter.** 2001. Pseudorabies virus UL37 gene product is involved in secondary envelopment. J. Virol. **75:**8927–8936.
36. **Klupp, B. G., C. J. Hengartner, T. C. Mettenleiter, and L. W. Enquist.** 2004. Complete, annotated sequence of the pseudorabies virus genome. J. Virol. **78:**424–440.
37. **Klupp, B. G., B. Lomniczi, N. Visser, W. Fuchs, and T. C. Mettenleiter.** 1995. Mutations affecting the UL21 gene contribute to avirulence of pseudorabies virus vaccine strain Bartha. Virology **212:**466–473.
38. **Kopp, M., H. Granzow, W. Fuchs, B. Klupp, and T. C. Mettenleiter.** 2004. Simultaneous deletion of pseudorabies virus tegument protein UL11 and glycoprotein M severely impairs secondary envelopment. J. Virol. **78:**3024–3034.
39. **Kopp, M., H. Granzow, W. Fuchs, B. G. Klupp, E. Mundt, A. Karger, and T. C. Mettenleiter.** 2003. The pseudorabies virus UL11 protein is a virion component involved in secondary envelopment in the cytoplasm. J. Virol. **77:**5339–5351.
40. **Kopp, M., B. G. Klupp, H. Granzow, W. Fuchs, and T. C. Mettenleiter.** 2002. Identification and characterization of the pseudorabies virus tegument proteins UL46 and UL47: role for UL47 in virion morphogenesis in the cytoplasm. J. Virol. **76:**8820–8833.
41. **Mettenleiter, T. C.** 1989. Glycoprotein gIII deletion mutants of pseudorabies virus are impaired in virus entry. Virology **171:**623–625.
42. **Mettenleiter, T. C.** 2000. Aujeszky's disease (pseudorabies) virus: the virus and molecular pathogenesis—state of the art, June 1999. Vet. Res. **31:**99–115.
43. **Mettenleiter, T. C.** 2002. Herpesvirus assembly and egress. J. Virol. **76:**1537–1547.
44. **Mettenleiter, T. C.** 2003. Pathogenesis of neurotropic herpesviruses: role of viral glycoproteins in neuroinvasion and transneuronal spread. Virus Res. **92:**197–206.
45. **Mettenleiter, T. C., and I. Rauh.** 1990. A glycoprotein gX-beta-galactosidase fusion gene as insertional marker for rapid identification of pseudorabies virus mutants. J. Virol. Methods **30:**55–65.
46. **Paxinos, G., and K. B. J. Franklin.** 2000. The mouse brain in stereotaxic coordinates, 2nd ed. Academic Press, Inc., San Diego, Calif.

46a. **Pomeranz, L. E., A. E. Reynolds, and C. J. Hengartner.** 2005. Molecular biology of pseudorabies virus: impact on neurovirology and veterinary medicine. Microbiol. Mol. Biol. Rev. **69:**462–500.

47. **Sabin, A. B.** 1938. Progression of different nasally instilled viruses along different nervous system pathways in the same host. Proc. Soc. Exp. Biol. Med. **38:**270–275.
48. **Sams, J. M., A. S. Jansen, T. C. Mettenleiter, and A. D. Loewy.** 1995. Pseudorabies virus mutants as transneuronal markers. Brain Res. **687:**182–190.
49. **Shankland, W. E.** 2000. The trigeminal nerve. Part I: an over-view. Cranio **18:**238–248.
50. **Tirabassi, R. S., R. A. Townley, M. G. Eldridge, and L. W. Enquist.** 1997. Characterization of pseudorabies virus mutants expressing carboxy-terminal truncations of gE: evidence for envelope incorporation, virulence, and neurotropism domains. J. Virol. **71:**6455–6464.
51. **Tomishima, M. J., and L. W. Enquist.** 2002. In vivo egress of an alphaherpesvirus from axons. J. Virol. **76:**8310–8317.